SPIE. The international society for optics and photonics

Search

ABOUT   CONFERENCES + EXHIBITIONS   **PUBLICATIONS**   MEMBERSHIP   INDUSTRY RESOURCES   EDUCATION   NEWS + VIDEOS

Print   Email   Share

◂ Conference Proceedings

Browse by Volume Number
Browse by Conference
Browse by Year

SPIE Journals

SPIE Digital Library

Books

Open Access

Contact SPIE Publications

Sign up for monthly alerts of new titles released.

Subscribe

PROCEEDINGS PAPER • NEW

A new insight on the distance averaging method: linear scanning versus matrix scanning

Author(s): Liliana Anchidin; Claudia-Alina Ilie; Stefania Bucuci; Razvan D. Tamas; George Caruntu

FORMAT	MEMBER PRICE	NON-MEMBER PRICE	
PDF	$14.40	$18.00	**ADD TO CART**

Paper Abstract

Antenna gain can be measured in a multipath site by moving the antenna under test away from the probe antenna at different distances, and by assessing a normalized transfer function as an average figure over the entire data set. In an earlier work, we provided a statistical explanation to the reduction of the multipath effects. Another possible explanation is based on the synthetic aperture principle, by assimilating the positions of the probe antenna to an

A New Insight on the Distance Averaging Method: Linear Scanning versus Matrix Scanning

Liliana Anchidin [1], Claudia-Alina Ilie [2], Stefania Bucuci [3],
Razvan D. Tamas[1], George Caruntu [1]

1) Department of Electronics and Telecommunications, Constanta Maritime University, Constanta, Romania
2) Department of Telecommunications, University Politehnica of Bucharest, Romania
3) Institut d'Electronique et Télécommunications de Rennes, France

ABSTRACT

Antenna gain can be measured in a multipath site by moving the antenna under test away from the probe antenna at different distances, and by assessing a normalized transfer function as an average figure over the entire data set. In an earlier work, we provided a statistical explanation to the reduction of the multipath effects. Another possible explanation is based on the synthetic aperture principle, by assimilating the positions of the probe antenna to an antenna array. In this paper, we compare linear scanning to matrix scanning in order to draw optimal choice criteria for the grid of measuring positions. Measurements were performed on a Vivaldi antenna.

Keywords: Antenna gain, multipath site, averaging method, synthetic aperture principle.

1. INTRODUCTION

In a previous work [1], we proposed a method for antenna gain evaluation in a multipath site. Basically, our method aims to reduce the effects of the indirect paths including reflection and diffraction on environing objects by measuring normalized transfer functions at different distances between the antenna under test (AUT) and the probe antenna and eventually, by calculating an average over that data set. The transfer functions are normalized by compensating the effect of the propagation as it would be in the free space, in terms of attenuation and delay.

Further work was focused on assessing the accuracy of our approach by comparing the results to those measured inside an anechoic chamber [2]. We showed that averaging can also relax the field zone constraints by properly defining a set of weighting functions [3], [4].

The theory of the method as presented in our previous work [1] shows how continuously distance-averaged data converges asymptotically to a free space result for a set of basic cases of reflection and diffraction. Although multipath transmission in a real measuring system is more complex it can imaginary be expanded in a series of such basic cases. It is straightforward that by moving away one of the antennas the effect of the indirect paths statistically cancels out and only the direct path has a constant, deterministic contribution regardless the distance.

In practice, the distance increment between two measuring positions cannot be set infinitely small, as considered in our early theoretical work; even a discrete, oversampled approach might not be practical as it yields a large data volume, especially when more than one direction of radiation is concerned. That is, the distance increment should be kept reasonable but carefully correlated to the effectiveness of the multipath effect cancelation.

In this paper, we provide a new insight on the distance averaging method by exploiting the similarity to the concept of synthetic aperture [5], mainly applied in radar signal processing [6]. The synthetic aperture approach not only provides an alternative, physical explanation to the reduction of the multipath effect, but it also provides one with an effective model for optimizing the spacing between the measuring positions. Broadside directive linear scanning has been previously used in compact range measuring systems in order to remove multipath effects [5]. In this work, we propose an end-fire directive scanning approach and we compare linear scanning to matrix scanning.

2. THEORY

Let us consider a set of two antennas, one of them in transmission mode and the other one in receiving mode (Fig. 1).
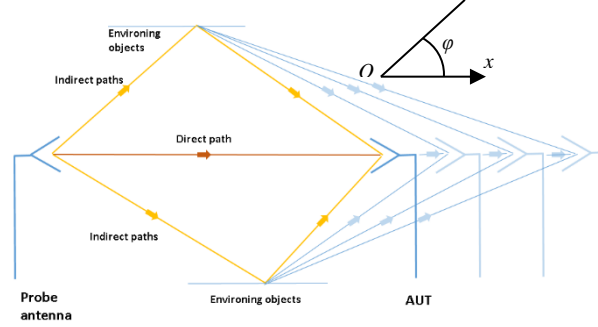

Fig. 1Distance averaging method: 1D approach.

An average transfer function can be derived from the scattering parameters $S_{21,n}$ measured for a set of N distances, $\{d_n\}$ between antennas by compensating the propagation effects i.e., attenuation and delay,

$$\overline{S_{21}} = \frac{1}{N} \sum_{n=1}^{N} \frac{d_n}{d_0} \cdot S_{21,n} \cdot \exp(jk_0 d_n) \tag{1}$$

where d_0 is the reference distance (usually set at 1 m).

In the analysis of an antenna gain, we have to take into account the dissipated losses as heat and provided from the system mismatch (Fig.2).
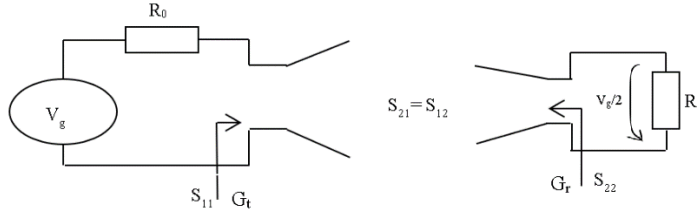

Fig. 2 Transmission between two antennas: calibrated - antenna under test (AUT).

Considering the system setup (Fig.2) we define an output voltage on the receiving antenna in terms of the transfer impedance Z_{21} and the mutual impedance on the receiving antenna Z_{22}.

$$V_2 = Z_{21}I_1 + Z_{22}I_2 \Rightarrow Z_{21} = \left.\frac{V_2}{I_1}\right|_{I_2=0} \tag{2}$$

The transfer parameters, S_{21} are found from ratio between the receiving antenna voltage and transmitted voltage

$$S_{21} = \left.\frac{b_2}{a_1}\right|_{a_2=0} = \frac{2V_2}{V_g} \tag{3}$$

The maximum power of transmission antenna (Fig.3)

$$P_t = \frac{1}{2} \frac{\left(\frac{V_g}{2}\right)^2}{R_0} (1 - |S_{11}|^2) \tag{4}$$

where $(1 - |S_{11}|^2)$ is represented the mismatch impedance at the input terminals of the transmitting antenna.

Ratio between reflected power and injected power is given in term of the power waves.

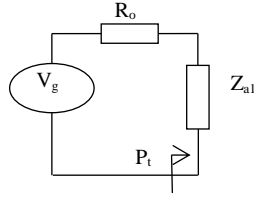$$\frac{P_{refl}}{P_{dir}} = \left|\frac{b_1}{a_1}\right|^2 \tag{5}$$

Fig. 3 The equivalent circuit for the transmitting antenna.

If antenna radiation resistance is adapted to an internal generator resistance ($Z_{a1} = R_0$), we find the transmitted voltage at the antenna terminals (Fig.4)

$$V_t = \frac{R_0}{2R_0}V_g = \frac{V_g}{2} \tag{6}$$

and the power (fig. 4) delivered for radiation

$$P_{in} = \frac{1}{2}\frac{\left(\frac{V_g}{2}\right)^2}{R_0}. \tag{7}$$
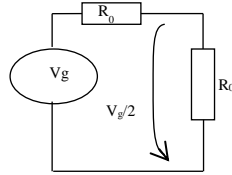

Fig. 4 The equivalent circuit of the transmission matched antenna.
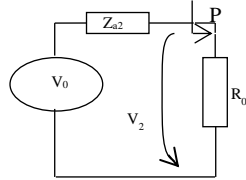
Figure 5 shows the antenna under test equivalent circuit

Fig. 5 The AUT equivalent circuit.

The antenna under test voltage is described

$$V_2 = V_0 \frac{R_0}{Z_{a2}+R_0} \tag{8}$$

where Z_{a2} is the antenna under test radiation impedance, and the power in this case is

$$P_2 = \frac{1}{2}\frac{V_2^2}{R_0} \tag{9}$$

The reflection coefficient, S_{22} yield the form

$$S_{22} = \frac{Z_{a2}-R_0}{Z_{a2}+R_0} \tag{10}$$

and

$$1 - S_{22} = 1 - \frac{Z_{a2}-R_0}{Z_{a2}+R_0} = \frac{2R_0}{Z_{a2}+R_0} \tag{11}$$

By substituting (8) and (11) the power is written

$$V_2 = \frac{V_0}{2}(1 - S_{22}) \tag{12}$$

and the power provided from the head delivered on the R_0 resistance is defined

$$P_{out} = \frac{1}{2}\frac{V_2^2}{R_0} = \frac{1}{2}\frac{\left(\frac{V_0}{2}\right)^2}{R_0}|1-S_{22}|^2 \tag{13}$$

The power reflected in respect with the power transmitted defined from Friis transmission formula

$$\frac{P_r}{P_t} = G_t G_r \left(\frac{\lambda}{4\pi r}\right)^2 \tag{14}$$

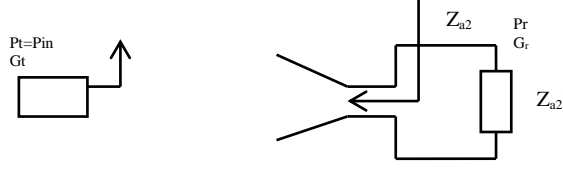Fig. 6 Transmission between two antennas considering Friis transmission equation.

In receiving mode, the antenna has a reactance X_{a2}. Then the power delivered to the receiver is maximum when the antenna reactance is the complex conjugate of the receiver's input reactance X_{a2}^*.

$$P_r = \frac{1}{2}\frac{\left(\frac{V_0}{2}\right)^2}{R_{a2}} \tag{15}$$

$$P_r = P_{out}\frac{R_0}{R_{a2}}\frac{1}{|1-S_{22}|^2} = \frac{V_2^2}{2R_0}\frac{R_0}{R_{a2}}\frac{1}{|1-S_{22}|^2} \tag{16}$$

Then the power ratio is

$$\frac{P_r}{P_t} = \frac{V_2^2}{2R_{a2}}\frac{1}{|1-S_{22}|^2}\frac{2R_0}{\left(\frac{V_g}{2}\right)^2(1-|S_{11}|^2)} \tag{17}$$

however

$$\frac{V_2^2}{\left(\frac{V_g}{2}\right)^2} = \left(\frac{2V_2}{V_g}\right)^2 = |S_{21}|^2 \tag{18}$$

By substituting (16) and (17) we rewrite in terms of power,

$$\frac{P_r}{P_t} = \frac{R_0}{R_{a2}(f)}\frac{|S_{21}|^2}{|1-S_{22}|^2(1-|S_{11}|^2)} \tag{19}$$

The gain of the receiving antenna is then found from the Friis transmission formula after elementary manipulations by taking into account possible impedance mismatches at both antennas, provided that all distances between antennas are in far-field zone [4].

$$G_r = \frac{1}{G_t}\left(\frac{4\pi r}{\lambda}\right)^2\frac{R_0}{R_{a2}(f)}\frac{|S_{21}|^2}{|1-S_{22}|^2(1-|S_{11}|^2)} \tag{20}$$

In (20), R_0 stands for the normalizing impedance (usually set at 50 ohms) and R_a is the radiation resistance of the antenna under test.

Moving one antenna away from the other is actually equivalent to using a linear, highly directive probe array instead of a single probe (usually omnidirectional). It comes out from relation (1) that the equivalent array is an endfire one [6] with an array factor

$$AF_{1D}(\phi) = \left|\sum_n I_n \cdot \exp\left(j\psi_n\right)\cdot\exp\left(-jk_0 d_n \cos\phi\right)\right| \tag{21}$$

where φ is the azimuth angle, provided that the AUT is moved away along the *Ox* axis. In our case, $I_n=1$ and $\psi_n= k_0 d_n$.

In order to reduce the effect of indirect paths on antenna measurements formation of large side lobes should be avoided. For 1*D*, endfire arrays large side lobes usually occur when the spacing between two radiating elements exceeds $\lambda/2$. As an example, with a spacing of 10 cm one should expect side lobes at above 1.5 GHz.

4

We calculated and compared the antenna factors for two arrays: a 1D, endfire array of 6 elements with a 10 cm spacing in-between along the *Ox* axis, and a 2D array of 6 by 3 elements with a 10 cm spacing in-between both along the *Ox* and *Oy* axis, respectively. The array factor can then be derived as

$$AF_{2D}(\phi) = \left| \sum_m I_{y,m} \cdot \exp\left(j\psi_{y,m}\right) \cdot \exp\left(-jk_0 d_{y,m} \sin\phi\right) \right|$$
$$\times \left| \sum_n I_{x,n} \cdot \exp\left(j\psi_{x,n}\right) \cdot \exp\left(-jk_0 d_{x,n} \cos\phi\right) \right| \quad (22)$$

where the distances along the *Ox* axis and the *Oy* axis between the field point and the measuring position indexed by (*m, n*) were denoted by $d_{x,n}$ and $d_{y,m}$, respectively. In order to provide a main lobe along the *Ox* axis we chose

$$I_{x,n} = I_{y,m} = 1,$$

$$\psi_{x,n} = k_0\, d_{x,n},$$

$$\text{and } \psi_{y,n} = 0.$$

Fig. 7 shows the array factor as a function of the azimuth angle for both arrays, at frequencies between 800 MHz and 2GHz.

As expected, large side lobes occur at above 1.5 GHz for the 1D array with a 10 cm spacing between measuring positions. Conversely, the 2D array not only provides a narrower main lobe, but it also exhibits much smaller side lobes, even at 2 GHz.
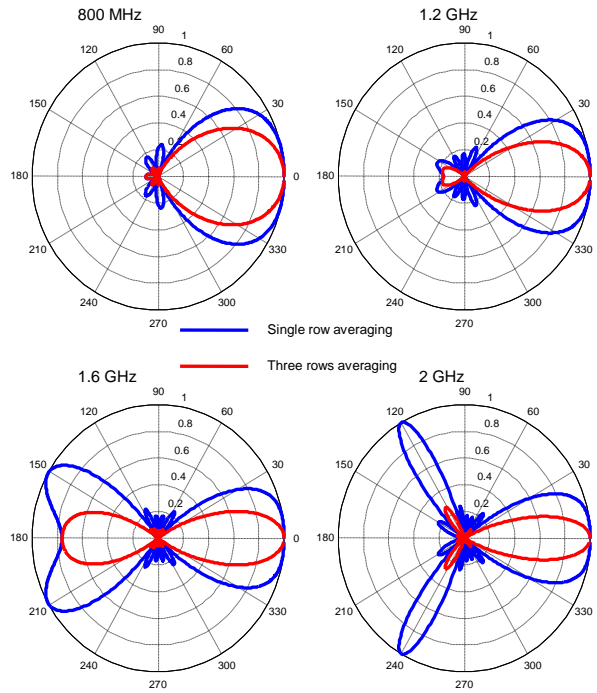

Fig. 7 Array factor for a 1D configuration: row with 6 measuring positions, distance increment of 10 cm along Ox. Array factor for a 2D configuration: matrix of 6 by 3 positions, distance increment of 10 cm both along Ox and Oy.

3. RESULTS

We consider a setup consisting of an antenna under test, a probe antenna, and a vector network analyzer. Measurements were performed in a multipath environment i.e., a regular room inside an office building. The antenna under test was a Vivaldi dipole (Fig. 8a) that operates at frequencies of above 500 MHz. A calibrated, biconical dipole was employed as a probe antenna (Fig. 8b).

a)   b)

Fig.8 Experimental setup: antenna under test (a), and probe antenna (b).

We measured the AUT gain by placing it into two configurations. The first configuration consisted of a row of 6 measuring positions with a distance increment along *Ox* of 10 cm and a minimal distance of 1 m between the probe and the AUT. The second configuration (Fig. 9) consisted of a matrix of 6 by 3 positions with a distance increment of 10 cm both along *Ox* and *Oy* axis, and a minimal distance of 1 m between the probe and the AUT.
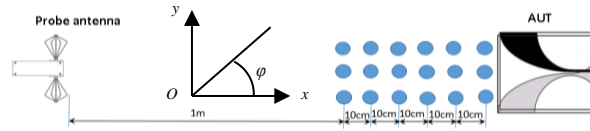

Fig. 9 Distance averaging method: 2D approach.

Figure 10 shows the gain of the AUT as a function of frequency for θ=90º and φ=0, extracted both with matrix and row configuration; simulated and measured gain are also given on the same diagram.
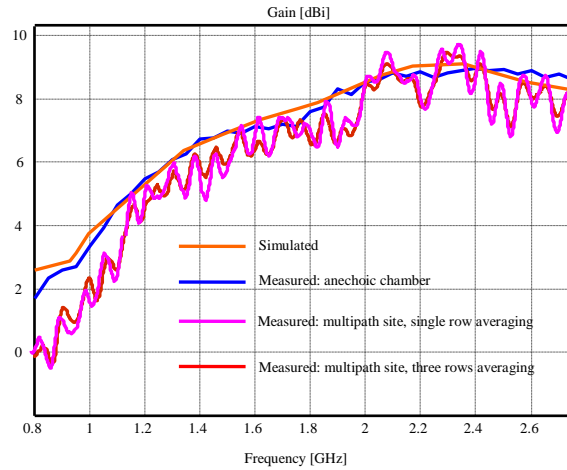

Fig. 10 Gain of the antenna under test for θ=90º and φ=0.

4. CONCLUSION

We compared gain results issued from measurements performed in a row configuration of 6 positions, and in a matrix configuration of 6 by 3 positions, respectively. The matrix configuration provides a ripple reduction by up to 1 dB, since the directivity of the virtual array improves and the multipath effect is therefore reduced. No field-zone correction was performed on the measured data, as the aim was to only investigate the effect of the multipath transmission; that explains discrepancies (other than ripples) between the results of our method and the gain measured in anechoic chamber with a multiprobe, professional system and near-field to far-field transformations.

It should be emphasized that even for matrix and row configurations with the same number of measuring positions and for a given range of AUT displacement the matrix arrangement would provide a narrower main lobe, as the beamwidth is mainly a function of the array size and not of the number of positions. The matrix configuration takes further advantage over the row configuration as it does not yield large side lobes when the spacing between two measuring positions exceeds half-wavelength.

Further work will focus on designing a platform for automatic, optimal positioning of the probe antenna for antenna gain measurements inside a multipath site.

Acknowledgements

References

[1] Tamas, R.D., Deacu, D., Vasile,G., and Ioana, C., "A method for antenna gain measrements in nonanechoic sites", Microwave and Optical Technology Letters, vol. 56, pp. 1553-1557 (2014).

[2] Deacu, D., Petrescu, T., Candel, I., and Petrut, T., "On the Accuracy of the Distance-Averaging Method for Antenna Gain Measurements", Proc. IEEE International Workshop on Antenna Technology, pp. 371-374 (2014).

[3] Anchidin, L., Tamas, R.D., Androne, A., and Caruntu, G., "Antenna Gain Evaluation Based on Weighting Near-Field Measurements", Proc. IEEE International Workshop on Antenna Technology, pp. 78-81 (2017).

[4] Anchidin, L. , Bari, F., Tamas, R.D., Pometcu, L., and Sharaiha, A., "Near-Field Gain Measurements: Single-Probe Distance Averaging in a Multipath Site versus Multi-Probe Field Scanning inside an Anechoic Chamber", Proc. 32nd URSI General Assembly and Scientific Symposium (2017).

[5] Li, H.-J., Liu, T.-Y., and Leou, J.-L., "Antenna Measurments in the presnce of multipath waves", Progress in Electromagnetics research, PIER 30, 157-178 (2001).

[6] Moreira, A., Prats-Iraola, P., Younis, M., Krieger, G., Hajnsek, I., and Papathanassiou, K. P., "A tutorial on synthetic aperture radar", IEEE Geoscience and Remote Sensing Magazine, vol. 1, pp. 6-43 (2013).

[7] Balanis, C. A., Antenna Theory - Analysis and Design, 3rd ed., New York: Wiley, pp.313-317 (2005).